ISSN 0023-1584, Kinetics and Catalysis, 2018, Vol. 59, No. 5, pp. 628–634. © Pleiades Publishing, Ltd., 2018.

Selective Catalytic Reduction of NO by NH_3 over MoO_3 Promoted Fe_2O_3 Catalyst[1]

J. Wang[a], Zh. Xu[a], W. Zhao[a], and X. Li[a, *]

[a]State Key Laboratory Breeding Base of Coal Science and Technology Co-founded by Shanxi Province and the Ministry of Science and Technology, Taiyuan University of Technology, Shanxi, Taiyuan 030024 P.R. China

**e-mail: lixiaoliang@tyut.edu.cn*

Received November 4, 2017

Abstract—A series of MoO_3 doped Fe_2O_3 catalysts prepared by the co-precipitation method were investigated in the selective catalytic reduction of NO by NH_3 (NH_3-SCR). The catalysts displayed excellent catalytic activity from 225 to 400°C and high tolerance to SO_2/H_2O poisoning at 300°C. To characterize the catalysts the N_2-BET, XRD, Raman, NO-TPD, NH_3-TPD and in situ DRIFTS were carried out. It was found that the main reason explaining a high NH_3-SCR performance might be the synergistic effect between Fe and Mo species in the catalyst that could enhance the dispersion of Fe_2O_3 and increase NH_3 adsorption on the catalyst surface.

Keywords: NO, NH_3-SCR, MoO_3 modified catalysts, synergistic effect

DOI: 10.1134/S002315841805018X

INTRODUCTION

Nitrogen oxides NO_x, produced by the combustion of fossil fuel, could cause many environmental issues, such as acid rain, ozone depletion and photochemical smog [1, 2]. The selective catalytic reduction of NO by NH_3 (NH_3-SCR) is the state-of-art technology for the NO_x abatement. For the coal fired power plants, the V_2O_5–WO_3 (MoO_3)/TiO_2 has been put into real application for many years due to its high De–NO_x efficiency and excellent tolerance to SO_2 poisoning. However, a narrow reaction temperature window of 300–400°C and the biological toxicity of vanadium species to the environment and human beings are some drawbacks of these catalysts [3, 4]. The development of the environmentally benign NH_3-SCR catalyst that can maintain promising catalytic performance has received increased attention in recent years.

The investigation of iron based oxide catalysts remains an active area of research because these materials exhibit a high level of the NH_3-SCR activity, high resistance to the SO_2 poisoning, environmentally friendly and relatively high redox properties. However, the NO conversion over pure Fe_2O_3 is far from satisfactory at low temperatures since iron oxide shows a relatively low surface area and acidity. To improve its NH_3-SCR performance, iron oxides have been doped with different promoters such as Fe–Ti [5], Fe–V [6], Fe–W [7, 8], Fe–Mn [9, 10], Fe–V–Ti [11] and Fe–Ce [12], all of which showed high NH_3-SCR performance under the conditions used in the catalytic testing. Therefore, it could be a good choice to introduce the suitable additive into the pure Fe_2O_3 to enhance its NH_3-SCR performance.

Alternatively, MoO_3 has been used as a promoter to improve the NH_3-SCR activity. MoO_3 modified $CeAlO_x$ showed high denitration efficiency and the redox ability with the total acidity of the catalyst enhanced by the introduction of Mo [13]. It was found that by adding MoO_3 into CeO_2/TiO_2 it is possible not only to increase the population of Brønsted acid sites but also reduce the thermal stability of the inactive nitrate species on the catalyst surface [14]. Meanwhile, Ding et al. reported that the introducing Mo to Ce–Zr mixed oxide catalyst could inhibit the growth of the CeO_2 particle size, improve the redox ability and increase the amount of surface Lewis acidity [15]. Based on the idea that iron based mixed oxide are highly active in the NH_3-SCR and MoO_3 exerts a positive promoting effect of in the denitration reaction the MoO_3 we have initiated the synthesis of modified Fe_2O_3 catalysts by co-precipitation method in order to compare the catalytic performance of these materials.

EXPERIMENTAL

Catalyst Preparation

MoO_3 modified Fe_2O_3 catalysts were synthesized by the co-precipitation method using $Fe(NO_3)_3 \cdot 9H_2O$ and $(NH_4)_6Mo_7O_{24} \cdot 5H_2O$ as precursors and 25 wt % $NH_3 \cdot H_2O$ as precipitator. The aqueous solu-

---

[1] The article is published in the original.

tions of $(NH_4)_6Mo_7O_{24} \cdot 5H_2O$ with equal weight $H_2C_2O_4 \cdot 2H_2O$ were added to deionized water. After the $(NH_4)_6$ $Mo_7O_{24} \cdot 5H_2O$ was dissolved completely, the $Fe(NO_3)_3 \cdot 9H_2O$ was added into the aqueous solution with required molar ratio (Fe/Mo = 1 : 1, 2 : 1, 4 : 1 and 8 : 1). Excessive 25 wt % $NH_3 \cdot H_2O$ solution was dropped into the mixed solution under vigorous agitation until pH 10. The precipitated solids were collected by filtration and washed with distilled water, followed by drying at 105°C for 12 h and subsequently calcination at 500°C for 5 h in the static air atmosphere. Finally, the catalyst pellets were crushed and sieved and an aliquot of the 40–60 mesh fraction was used in further experiments. For comparison purpose, pure Fe_2O_3 and MoO_3 were also prepared using the same synthetic method.

Characterization of Catalysts

The specific surface area, pore volume and the average pore size of the samples were obtained by N_2 adsorption/desorption at 77 K using a Micromeritics Tristar-3000 system (Micromeritics, US). The crystallinity of the catalysts were measured by means of powder XRD patterns obtained on a Rigaku D/max 2500 X-ray diffractometer (Rigaku, Japan) with CuK_α radiation. Visible Raman spectra were registered at room temperature on a Spex 1877 D triplemate spectrograph (HORIBA Jobin Yvon, France) with spectral resolution of 2 cm^{-1}. NO-TPD and NH_3-TPD profiles were measured by the Autosorb-iQ-C chemisorption analyzer (Quantachrome Instruments, US). Prior to NO-TPD the sample was first pretreated in a flow of He at 400°C for 1 h and then cooled to 100°C. Afterwards, the sample was exposed to a flow of 500 ppm NO for 1 h, followed by He purge for 1 h. Finally, NO-TPD was run by heating the samples in He from 100 to 600°C at 10°C/min. In the case of NH_3-TPD, the samples were pretreated at 400°C under He for 1h, then cooled to 50°C and saturated with 10% NH_3/He for 1 h, followed by purging with He for 30 min. Finally, the samples were heated from 50 to 600°C at a rate of 10°C/min. The in situ DRIFTS experiments were performed on a Fourier transform infrared (FT-IR) spectrometer (Nicolet Nexus 670, (Nicolet, US) equipped with an in situ diffuse reflection chamber and high sensitivity mercury-cadmium-telluride (MCT) detector.

Activity Test

A fixed bed reactor was used to evaluate the NH_3-SCR activity. The flue composition was as follows: 500 ppm NO, 500 ppm NH_3, 5% O_2, 5 vol % H_2O (when used), 100 ppm SO_2 (when used), N_2 flow into balance and a total flow rate of 500 mL/min. To maintain the GHSV at 50000 h^{-1} a fixed volume of the catalyst (0.6 mL) was used. The concentrations of NO and NO_2 in the inlet and outlet gas were quantitatively measured with an online chemiluminescent NO/NO_x analyzer (KM9106, Kane Inc., UK) and the N_2O concentration was analyzed by a gas chromatograph (FULI 9790, Zhejiang Wenling Inc., China) with a porapak Q column. NO conversion and N_2O selectivity were calculated by using:

$$\text{NO conversion} = \frac{[NO_x]_{in} - [NO_x]_{out}}{[NO_x]_{in}} \times 100\%,$$

$$N_2O \text{ selectivity} = \frac{2[N_2O]_{out}}{[NO_x]_{in} - [NO_x]_{out}} \times 100\%,$$

$$[NO_x] = [NO] + [NO_2].$$

RESULTS AND DISCUSSION

Activity Test

The NO conversion and N_2O selectivity in the selective catalytic reduction of NO by NH_3 as a function of temperature over Fe_2O_3, MoO_3 and MoO_3 modified Fe_2O_3 catalysts are shown in Fig. 1. It can be readily seen that pure MoO_3 exhibited negligible SCR activity and N_2O selectivity over the whole temperature range. Pure Fe_2O_3 also showed poor NH_3-SCR catalytic performance with the maximum NO conversion at 250°C not exceeding 32.6%. However, the NH_3-SCR activity could be improved markedly upon adding MoO_3 to Fe_2O_3. At the Fe/Mo molar ratio = 1 : 1, more than 40% of NO was converted and N_2O selectivity below 5% was achieved in the temperature range from 250 to 450°C. When the Fe/Mo molar ratio reached a value of 2 : 1, the SCR activity and N_2O selectivity was further improved over the whole temperature range used in the test. When the Fe/Mo molar ratio was increased to 4 : 1, the highest activity was attained in the tested temperature range, with the NO conversion >90% and N_2O selectivity <5%. However, further increasing the Fe/Mo molar ratio decreased the NO conversion at both low and high temperatures. Therefore, the activity was probably associated with the Fe/Mo molar ratio and the optimal ratio was 4 : 1.

For the purposes of evaluating the anti-poisoning tolerance to SO_2 and H_2O, the Fe_4MoO_x catalyst was selected to investigate the impact of 100 ppm SO_2 and/or 5 vol % H_2O on its catalytic performance at 300°C with the corresponding results collected in Fig. 2. It could be seen that the Fe_4MoO_x catalyst maintained nearly 100% NO conversion during the tested period in the present of 5 vol % of H_2O. When 100 ppm of SO_2 was injected into the reaction gases, the NO conversion decreased and gradually became stable. The NO conversion was recovered after removing SO_2. As the 100 ppm of SO_2 and 5 vol % H_2O were introduced into the reaction gases synchronously, the NO conversion decreased much more markedly,

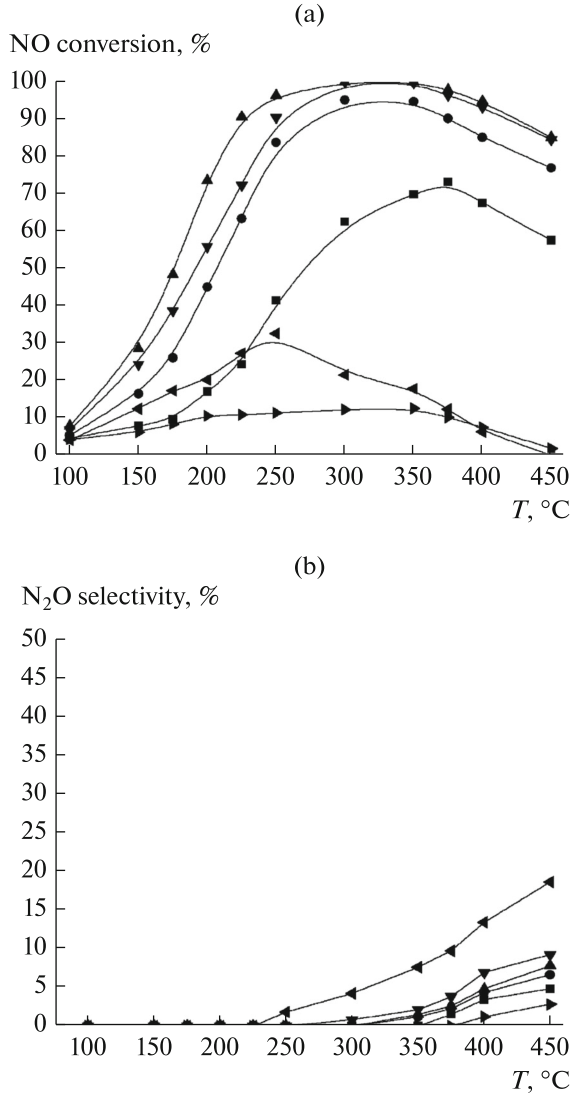

Fig. 1. NH_3-SCR activity (a) and N_2O selectivity (b) as function of temperature over Fe_2O_3, MoO_3 and MoO_3 modified Fe_2O_3 catalysts (■ Fe : Mo = 1 : 1, ● Fe : Mo = 2 : 1, ▲ Fe : Mo = 4 : 1, ▼ Fe : Mo = 8 : 1, ◀ Fe_2O_3, ▶ MoO_3) under GHSV of 50000 h^{-1}.

which could be attributed to the presence of NH_4HSO_4 deposited on the catalyst surface [15]. However, the NO conversion exceeded values of 89% during the tested period. All these results suggest that the catalyst showed an adequate tolerance to SO_2/H_2O poisoning.

BET Result

The BET physical property parameters of the Fe_2O_3, MoO_3 and Mo modified Fe_2O_3 catalysts are summarized in Table. It could be found that the BET surface area and pore volume of the Fe–Mo mixed oxide increased at first and then decreased with

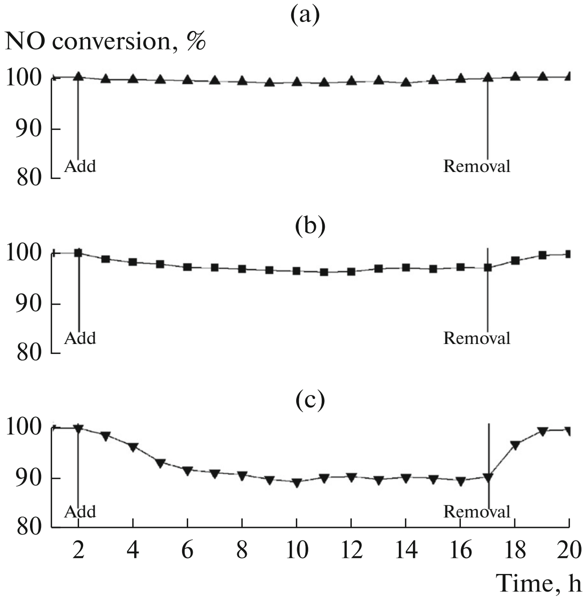

Fig. 2. NH_3-SCR activity over Fe_4MoO_x catalyst in the presence of H_2O/SO_2: (a) 5% H_2O, ▲; (b) 100 ppm SO_2, ■; (c) 5% H_2O + 100 ppm SO_2,▼. At 300°C under GHSV of 50000 h^{-1}.

increasing Fe/Mo molar ratio remaining however much larger than those found for pure Fe_2O_3 and MoO_3. This trend was also consistent with the variations in the NO conversion over the temperature range of 250–450°C. However, reductions in the average pore diameter associated with the addition of MoO_3 into the Fe_2O_3 catalyst cannot be correlated with the amount of the dopant. It could be therefore implied that the catalyst structural parameters are hardly the key factors determining the NH_3-SCR activity. Combining the NH_3-SCR performance and BET analysis results, it also could be suggested that incorporation of Mo into Fe oxide results in the formation of MoO_3 promoted Fe_2O_3 catalysts with properties different from a mechanical mixture of two oxides.

XRD and Raman Analysis

The presence of crystal phase of Fe_2O_3 in the MoO_3 modified Fe_2O_3 catalyst is confirmed by X-ray diffraction study (Fig. 3a). XRD patterns of all samples show characteristic broad peaks at 24.3°, 33.4°, 35.8°, 41.1°, 49.6°, 54.2°, 57.8°, 62.7°, 64.2°, 72.3° and 75.6° (2θ) corresponding to the typical Hematite-Fe_2O_3 (PDF33-0664). At the same time, no characteristic diffraction peaks of MoO_3 were observed. A weak crystallization or a good dispersion on the MoO_3 modified Fe_2O_3 surface may be a reason. Table 1 shows the crystallite sizes of Hematite-Fe_2O_3 in the tested catalysts calculated by using the Scherrer equa-

Table 1. The BET physical parameters of the MoO_3 modified Fe_2O_3 catalysts

Sample	BET surface area, m^2/g	BJH pore volume, cm^3/g	Average pore size, nm	Crystallite size of $Fe_2O_3^*$, nm
Fe_2O_3	42.4	0.23	17.1	22.7
$FeMoO_x$	64.9	0.36	10.3	19.6
Fe_2MoO_x	73.2	0.45	13.2	17.5
Fe_4MoO_x	82.7	0.58	14.4	14.1
Fe_8MoO_x	76.2	0.49	21.6	15.1
MoO_3	1.6	0.02	45.8	–

*Fe_2O_3 crystallite size calculated by Scherrer equation from XRD results.

tion. The data indicate variations in the crystallite dimensions of the catalyst samples prepared with different Fe/Mo molar ratio. The lower Hematite-Fe_2O_3 crystallite sizes were registered for the Fe_2O_3 catalysts containing increased amounts MoO_3. It can be thus inferred that the incorporation of molybdenum oxide decreases the crystallite size of Fe_2O_3 thus enhancing the dispersion of Fe_2O_3 on the catalyst surface.

For the purposes of further understanding of the structural characteristics, Raman spectroscopy was also employed with the corresponding results collected in Fig. 3b. As can be seen, the spectrum of MoO_3 showed nine Raman bands at 116, 129, 158, 284, 337, 378, 665, 819 and 995 cm^{-1} [16, 17]. In the spectrum of Fe_2O_3 four bands at 215, 281, 391 and 587 cm^{-1} could be observed assignable to hematite with small differences in peak positions (±5 cm^{-1}) [18]. The band at 215 cm^{-1} is due to the Raman active A_{1g} mode of hematite and three peaks at 281, 391 and 587 cm^{-1} are ascribed to E_g modes of hematite [19]. No MoO_3 species were detected in the Fe–Mo based catalysts. In addition, the band intensities due to Fe_2O_3 on Fe–Mo mixed oxides decreased, indicating that doping with Mo inhibited the crystallization of Fe_2O_3 phase. Given that crystalline MoO_3 could be otherwise easily detected on the catalyst surface by using Raman spectrum, the absence of the signals corresponding to MoO_3 crystalline phase on the MoO_3 modified Fe_2O_3 catalysts suggests a high degree of dispersion of MoO_3 species on the catalyst surface. The corresponding analytical data are in good agreement with the XRD results.

NO-TPD and NH_3-TPD Analysis

The NO adsorption on the Fe_2O_3, MoO_3 and Fe_4MoO_x catalysts was characterized by using NO-TPD with the corresponding results presented in Fig. 4a. Fe_2O_3 and Fe_4MoO_x had two desorption peaks, whereas for MoO_3 no peak was observed in the spectra. Desorption peaks at 210°C for Fe_4MoO_x and 245°C for Fe_2O_3 can be ascribed to the decomposition of bridging nitrate. Desorption peaks at 307°C for Fe_4MoO_x and 347°C for Fe_2O_3 are assigned to the decomposition of monodentate nitrate [17]. It appears that only sites associated with iron atoms are available for adsorption of NO over these three catalysts and the addition of MoO_3 on the Fe_4MoO_x could inhibit the formation of nitrate species to a certain degree. The inhibition may be related to a reduced thermal stability of the inactive nitrate specie on the catalyst surface [14]. Although adsorption power of the Fe_4MoO_x towards NO is weaker than that of the pure Fe_2O_3, doping with Mo markedly improved the NH_3-SCR activity. The above results imply that some synergetic effect between Mo and Fe species might exist in the catalyst and make a material contribution to the improvement of the NH_3-SCR performance.

The amount of acid sites on the catalyst surface plays a crucial role in the NH_3-SCR performance. The acid content on the catalysts surface is characterized by using NH_3-TPD with the corresponding profiles shown in Fig. 4b. It can be seen that the desorption curve for the Fe_2O_3 catalyst has two main peaks at 107 and 368°C. The peak at 107°C can be assigned to the weakly adsorbed NH_3, the peak at 368°C can be attributed to the strongly adsorbed NH_3 and the total acidity of the Fe_2O_3 catalyst was ~9.37 $\mu mol\ g^{-1} m^{-2}$. Notably, the intensity of the Fe_4MoO_x desorption peak was enhanced significantly by doping with Mo. The peak due to the strongly adsorbed NH_3 at 368°C was shifted at 409°C and the total acidity was increased to about 13.84 $\mu mol\ g^{-1} m^{-2}$. An explanation can be offered that ammonia was coordinatively bound to Mo surface cation species or protonated as NH_4^+ by interacting with Mo–OH groups on the catalyst surface [21]. It seems that the increase in the surface acidity is a key factor contributing to the improvement of the NH_3-SCR activity.

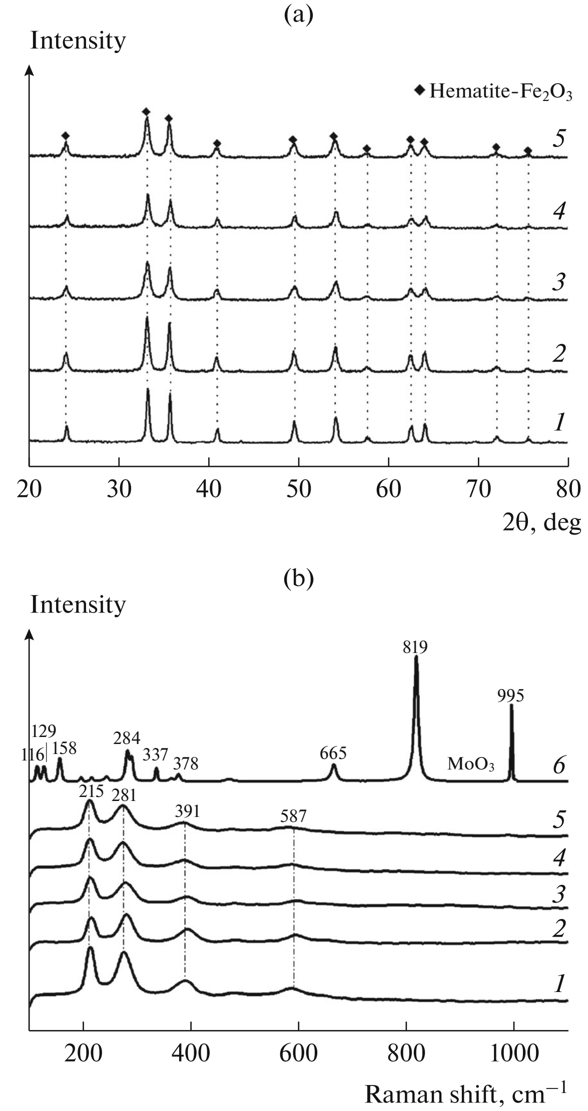

Fig. 3. (a) XRD profiles of the catalysts: (*1*) Fe_2O_3, (*2*) $FeMoO_x$, (*3*) Fe_2MoO_x, (*4*) Fe_4MoO_x, (*5*) Fe_8MoO_x. (b) Raman spectra of the catalysts: (*1*) Fe_2O_3, (*2*) $FeMoO_x$, (*3*) Fe_2MoO_x, (*4*) Fe_4MoO_x, (*5*) Fe_8MoO_x, (*6*) MoO_3, (λ_{ex} = 514.5 nm).

In situ DRIFTS Results Analysis

The in situ DRIFTS analysis was performed to study NH_3 adsorption and NO + O_2 adsorption on the MoO_3, Fe_2O_3 and Fe_4MoO_x catalysts at 200°C. According to the in situ DRIFTS information shown in Fig. 5, no bands could be observed after adsorption of NH_3 or NO + O_2 on the surface of MoO_3. When the sample of Fe_2O_3 was exposed to NH_3, several bands appeared at 1205, 1429, 1602, 3160, 3255, 3347, 3579, 3648 and 3724 cm^{-1}. The band at 1205/1602 cm^{-1} could be attributed to NH_3 coordinatively bound to Lewis acid sites [21, 22], while the band at 1420 cm^{-1} can be assigned to ionic NH_4^+ species on Brønsted acid sites [6]. The bands at 3160, 3255 and 3347 cm^{-1} due to N–H stretching vibration modes and three negative bands at 3579, 3648 and 3724 cm^{-1} caused by the surface O–H stretching were also observed [23–27]. After introducing NH_3 to the Fe_4MoO_x sample, the band attributable to ionic NH_4^+ species disappeared. However, the affinity of Lewis acid sites to NH_3 molecules strengthened evidently. In the N–H stretching region, three new bands were found at 3162, 3265 and 3349 cm^{-1}. In addition, another three negative bands appeared at 3632, 3655 and 3720 cm^{-1}, which could be assigned to absorption of hydroxyl groups. The NH_3 adsorption results were consistent with the NH_3-TPD testing data. After introducing NO + O_2 into the DRIFT cell, some bands appeared at 1203, 1215, 1350, 1548, 1566, 1595 and 1597 cm^{-1}. The bands at 1203

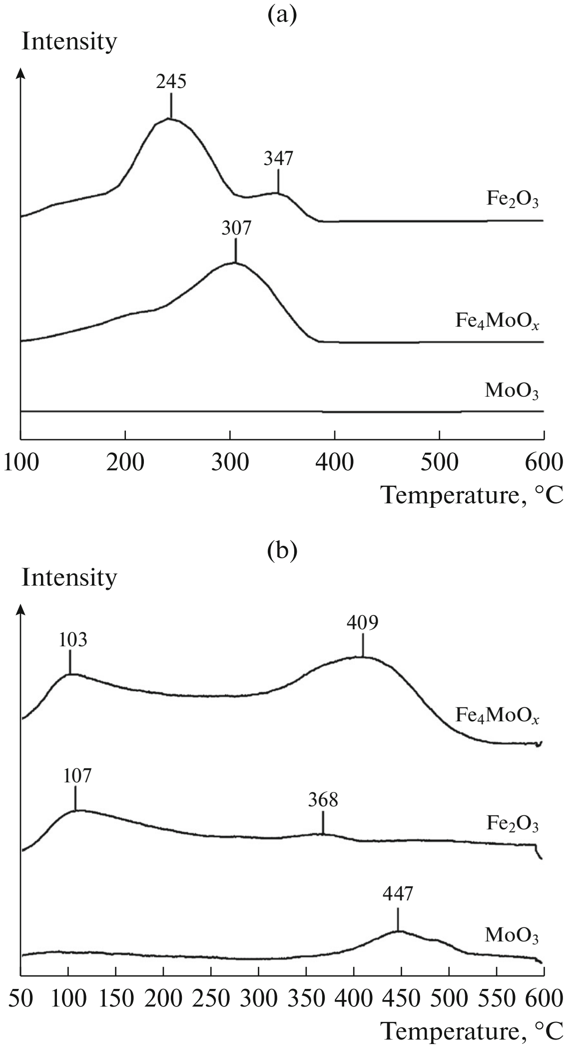

Fig. 4. NO-TPD (a) and NH_3-TPD (b) profiles of Fe_2O_3, MoO_3, and Fe_4MoO_x.

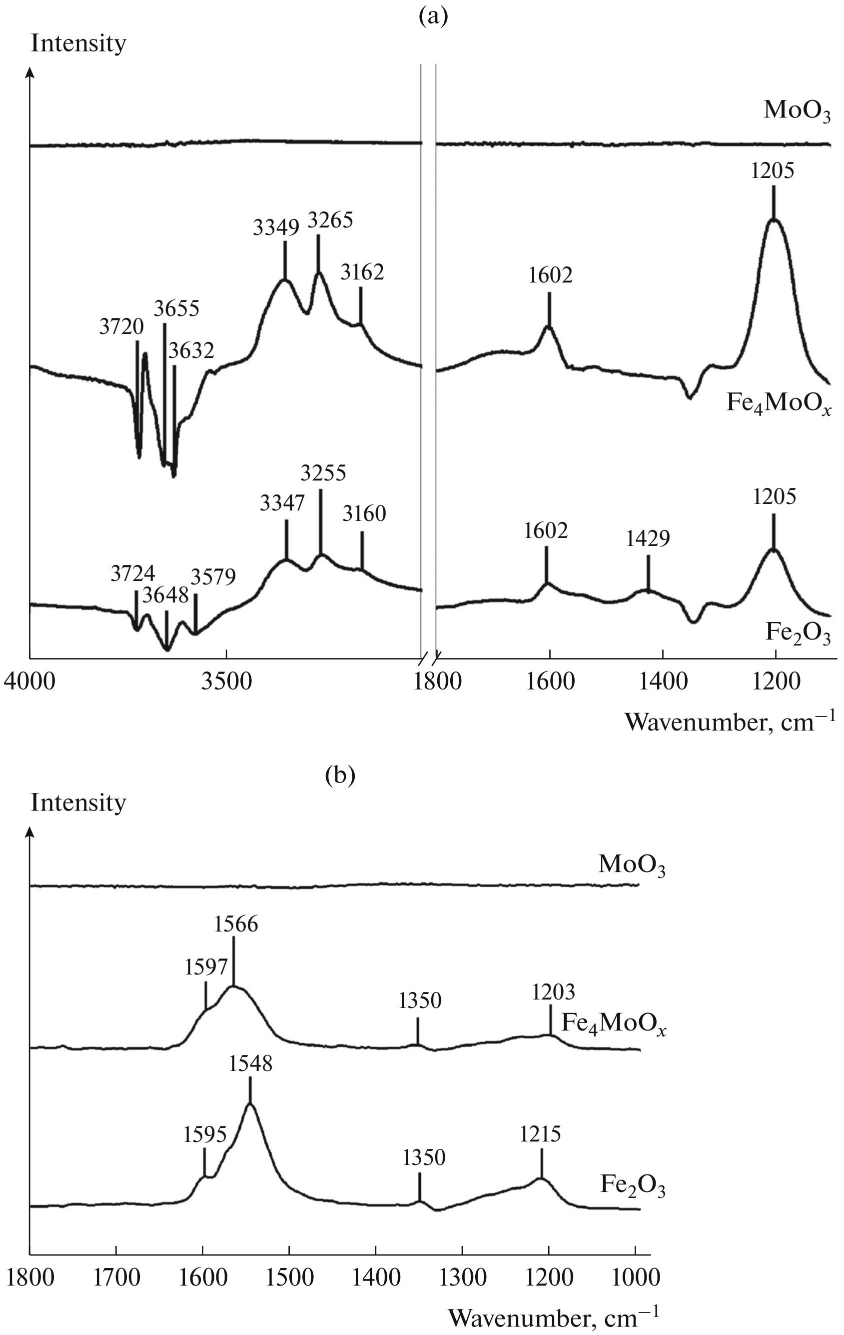

Fig. 5. In situ DRIFTS of NH_3 adsorption (a), NO + O_2 adsorption (b) on the Fe_2O_3, MoO_3, and Fe_4MoO_x catalyst at 200°C.

and 1350 cm^{-1} were assigned to chelated NO_2^- and chelating nitrites, respectively [28, 29]. The bands at 1215, 1595 and 1597 cm^{-1} are due to bridging nitrate species [30, 31], the bands attributable to monodentate nitrate were also found at 1548 and 1566 cm^{-1} [22, 32]. The intensity of the bands on the Fe_4MoO_x catalyst was slightly compared to those of Fe_2O_3 in agreement with the NO-TPD results. From the above analysis, the development of a certain synergistic effect between Fe and Mo species in the MoO_3 modified Fe_2O_3 catalysts can be postulated, which could strengthen the adsorption power of the catalyst surface to NH_3 and in this way enhance the de-NO_x activity.

In conclusion, MoO_3 modified Fe_2O_3 catalysts prepared by conventional co-precipitation method exhibited excellent NH_3-SCR activity over a relatively wide temperature range from 225 to 400°C and strong resistance to SO_2 and H_2O poisoning. The existence of the synergistic effect between Fe and Mo species in the

MoO_3 modified Fe_2O_3 catalyst was crucial for achieving an improved NH_3-SCR performance.

REFERENCES

1. Bosch, H. and Janssen, F., *Catal. Today*, 1988, vol. 2, p. 369.
2. Li, X., Li, X., Li, J., and Hao, J., *J. Hazard. Mater.*, 2016, vol. 318, p. 615.
3. Chen, L., Niu, X., Li, Z., Dong, Y., Zhang, Z., Yuan, F., and Zhu, Y., *Catal. Commun.*, 2016, vol. 85, p. 48.
4. Shan, W., Liu, F., Yu. Y., He, H., Deng, C., and Zi, X., *Catal. Commun.*, 2015, vol. 59, p. 226.
5. Liu, F., He, H., and Zhang, C., *Chem. Commun.*, 2008, vol. 17, p. 2043.
6. Zhang, P. and Li, D., *Catal. Lett.*, 2014, vol. 144, p. 959.
7. Li, X., Li, J., Peng, Y., Zhang, T., Liu, S., and Hao, J., *Catal. Sci. Technol.*, 2015, vol. 5, p. 556.
8. Liu, Z., Su, H., Chen, B., Li, J., and Woo, S., *Chem. Eng. J.*, 2016, vol. 299, p. 255.
9. Chen, Z., Wang, F., Li, H., Yang, Q., Wang, L., and Li, X., *Ind. Eng. Chem. Res.*, 2011, vol. 51, p. 202.
10. Yang, S., Wang, C., Li, J., Yan, N., Ma, L., and Chang, H., *Appl. Catal., B*, 2011, vol. 110, p. 71.
11. Liu, F., He, H., Lian, Z., Shan, W., Xie, L., Asakura, K., and Deng, H., *J. Catal.*, 2013, vol. 307, p. 340.
12. Han, J., Meeprasert, J., Maitarad, P., Nammuangruk, S., Shi, L., and Zhang, D., *J. Phys. Chem. C*, 2016, vol. 120, p. 1523.
13. Li, X. and Li, Y., *J. Mol. Catal. A: Chem*. 2014, vol. 386, p. 69.
14. Liu, Z., Zhang, S., Li, J., and Ma, L., *Appl. Catal., B*, 2014, vol. 144, p. 90.
15. Ding, S., Liu, F., Shi, X., Liu, K., Lian, Z., and Xie, L., *ACS Appl. Mater. Interfaces*, 2015, vol. 7, p. 9497.
16. Srilakshmi, C., Chew, W., Ramesh, K., and Garland, M., *Inorg. Chem.*, 2009, vol. 48, p. 1967.
17. Seguin, L., Figlarz, M., Cavagnat, R., and Lassègues, J.C., *Spectrochim. Acta, Part A*, 1995, vol. 51, p. 1323.
18. Wan, Y., Shi, X., Xia, H., and Xie, J., *Mater. Res. Bull.*, 2013, vol. 48, p. 4791.
19. Fan, H., You, G., Li, Y., Zheng, Z., Tan, H., Shen, Z., Tang, S., and Feng, Y., *J. Phys. Chem. C*, 2009, vol. 113, p. 9928.
20. Liu, F., He, H., Zhang, C., Shan, W., and Shi, X., *Catal. Today*, 2011, vol. 175, p. 18.
21. Lian, Z., Liu, F., He, H., Shi, X., Mo, J., and Wu, Z., *Chem. Eng. J.*, 2014, vol. 250, p. 390.
22. Yang, S., Xiong, S., Liao, Y., Xiao, X., Qi, F., Peng, Y., Fu, Y., and Shan, W., *Environ. Sci. Technol.*, 2014, vol. 48, p. 10354.
23. Busca, G., Larrubia, M.A., Arrighi, L., and Ramis, G., *Catal. Today*, 2005, vol. 107, p. 139.
24. Zhang, T., Liu, J., Wang, D., Zhao, Z., Wei, Y., Cheng, K., Jiang, G., and Duan, A., *Appl. Catal., B*, 2014, vol. 148, p. 520.
25. Liu, F., Asakura, K., He, H., Shan, W., Shi, X., Zhang, C., *Appl. Catal., B*, 2011, vol. 103, p. 369.
26. Chen, W., Qu, Z., Huang, W., Hu, X., and Yan, N., *Fuel*, 2016, vol. 166, p. 179.
27. Lónyi, F., Solt, H.E., Valyon, J., Decolatti, H., Gutierrez, L., and Miró, E., *Appl. Catal., B*, 2010, vol. 100, p. 133.
28. Peng, Y., Li, J., Huang, X., Li, X., Su, W., Sun, X., and Wang, D., *Environ. Sci. Technol.*, 2014, vol. 48, p. 4515.
29. Li, L., Qu, L., Cheng, J., Li, J., and Hao, Z., *Appl. Catal., B*, 2009, vol. 88, p. 224.
30. Schraml-Marth, M., Wokaun, A., and Baikert, A., *J. Catal.*, 1992, vol. 138, p. 306.
31. Liu, Z., Yi, Y., Zhang, S., Zhu, T., Zhu, J., and Wang, J., *Catal. Today*, 2013, vol. 16, p. 76.
32. Yang, S., Qi, F., Liao, Y., Xiong, S., Lan, Y., Fu, Y., Shan, W., and Li, J., *Ind. Eng. Chem. Res.*, 2014, vol. 53, p. 5810.